

# Magnetic field independence of Cu(2) NMR spin-lattice relaxation rate in the normal state of optimally doped $\text{YBa}_2\text{Cu}_3\text{O}_{7-\delta}$

K. R. Gorny,<sup>1</sup> O. M. Vyaselev,<sup>2</sup> C. H. Pennington,<sup>1</sup> P. C. Hammel,<sup>3</sup> W. L. Hults,<sup>3</sup> J. L. Smith,<sup>3</sup> J. Baumgartner,<sup>1</sup> T. R. Lemberger,<sup>1</sup> P. Klamut,<sup>4</sup> and B. Dabrowski<sup>4</sup>

<sup>1</sup>*Department of Physics, The Ohio State University, 174 West 18th Avenue, Columbus, Ohio 43210*

<sup>2</sup>*Institute of Solid State Physics, Chernogolovka 142432, Russia*

<sup>3</sup>*Los Alamos National Laboratory, Los Alamos, New Mexico 87545*

<sup>4</sup>*Department of Physics, Northern Illinois University, DeKalb, Illinois 60115*

(Received 5 July 2000; revised manuscript received 29 September 2000; published 22 January 2001)

We report NMR measurements of  $^{63}\text{Cu}$  spin-lattice relaxation rates,  $^{63}(T_1T)^{-1}$ , for magnetic fields of 0, 4, 8.8, and 14.8 T. The measurements were performed on four different samples within the family of near optimally doped  $\text{YBa}_2\text{Cu}_3\text{O}_{7-\delta}$  and for the range of temperatures above and below  $T_c$ . For each sample we consistently find that, in the normal state,  $^{63}\text{Cu}$  spin-lattice relaxation rate is magnetic field independent and that field dependence develops only *below*  $T_c$  where  $^{63}(T_1T)^{-1}$  curves “fan out.” We describe in detail experimental methods enabling the high precision required in such measurements.

DOI: 10.1103/PhysRevB.63.064513

PACS number(s): 74.72.Bk, 74.25.Nf, 74.40.+k, 76.60.-k

## I. INTRODUCTION

The behavior of the high-temperature superconductors near and above the superconducting transition remains an important subject of experiment, probing both fluctuation effects and the spin/charge gap. In particular, over the past several years, there has been a spirited dialog regarding the true behavior and field dependence of the  $^{63}\text{Cu}$  NMR spin-lattice relaxation rate  $^{63}(T_1T)^{-1}$  in optimally doped  $\text{YBa}_2\text{Cu}_3\text{O}_{7-\delta}$ .<sup>1-4</sup> Early reports<sup>1,2</sup> indicated peculiar field dependences in which the rate  $^{63}(T_1T)^{-1}$  as measured by NMR at fields 6–8 T differed substantially (with effects of order 15%) from the rate as measured by nuclear quadrupole resonance (NQR) at zero field. These effects were attributed variously to field suppression of “antiferromagnetic spin fluctuations”<sup>1</sup> or “the phase-sensitive Maki-Thompson effect.”<sup>2</sup> In contrast, our group<sup>3</sup> subsequently provided measurements of  $^{63}(T_1T)^{-1}$  from 0 to 15 T and found no field dependence above  $T_c$ , with an experimental precision of  $\sim 1\%$ . We suggested<sup>3</sup> that the apparent field dependences observed by the previous investigators resulted from certain artifacts related to their measurement techniques. Namely, the previous investigators made  $^{63}(T_1T)^{-1}$  measurements upon the “central” ( $\frac{1}{2}, -\frac{1}{2}$ ) transition of spin- $\frac{3}{2}$   $^{63}\text{Cu}$ . We discussed and demonstrated experimentally<sup>3</sup> that these measurements were susceptible to “background” contamination problems, and we employed a different measurement technique, using the “satellite” ( $\frac{3}{2}, \frac{1}{2}$ ) transitions, that we demonstrated to be free of these undesirable effects.

Subsequent to our work, however, Mitrovic *et al.*<sup>4</sup> employed a very different technique to infer the  $^{63}(T_1T)^{-1}$  and its field dependence. Namely, they observed the transverse relaxation rate ( $1/T_2$ ) of  $^{17}\text{O}$ , and employed a formalism developed by Recchia *et al.*<sup>5,6</sup> and Walstedt and Cheong<sup>7,8</sup> to infer the desired longitudinal relaxation rate  $^{63}(T_1T)^{-1}$  for  $^{63}\text{Cu}$ . As such, their method is an “indirect” technique, though it is not immediately clear that it could not yield accurate results. They found, for temperatures just above  $T_c$ , a nonmonotonic field dependence in which  $^{63}(T_1T)^{-1}$  varied

by as much as 20% over the range of fields 0–24 T. They interpreted their data in terms of a model of *d*-wave pairing and superconducting fluctuations.

Speculation<sup>9</sup> regarding the source of these experimental discrepancies centered on the possibility that the samples used by the various groups might be different in some way, despite the fact that all samples consisted of near-optimally doped  $\text{YBa}_2\text{Cu}_3\text{O}_{7-\delta}$ , with  $T_c$ 's above 90 K. However, Mitrovic *et al.* have since announced<sup>10</sup> that they find that their direct measurements of  $^{63}(T_1T)^{-1}$ , employing the satellite measurement technique that we used and advocated, yield no field dependence, in agreement with our results.

Now there is reasonable consensus that direct measurement of  $^{63}(T_1T)^{-1}$  yields no field dependence, and hence that the theories developed in response to apparent field dependences must be reconsidered. The anguished history of the topic though suggests that it is worthwhile to report here the experimental procedures that were developed to obtain the high precision methods of Ref. 3. We also report here the extension of the experiment to several more near optimally doped samples, in response to previous suggestions<sup>9</sup> that sample detail is crucial. We find that the conclusion of magnetic field independence of  $^{63}(T_1T)^{-1}$  is not sensitive to the detailed properties of the sample.

## II. SAMPLES

Our measurements were carried out on “aligned powder” samples commonly used in high- $T_c$  NMR. The samples were aligned in Stycast 1266 epoxy with the crystallite *c* axis parallel, following the detailed procedure described by Martindale.<sup>11</sup>

We report here on four samples. Sample A was prepared by the Smith/Hults Los Alamos team, and is the sample of Ref. 3. Sample A was enriched in  $^{17}\text{O}$  for purposes unrelated to this experiment. To aide the reader in keeping track of this sample, we refer to it as “sample A (Smith/Hults,  $^{17}\text{O}$  enriched).”

Sample B was also prepared by Smith/Hults and is the

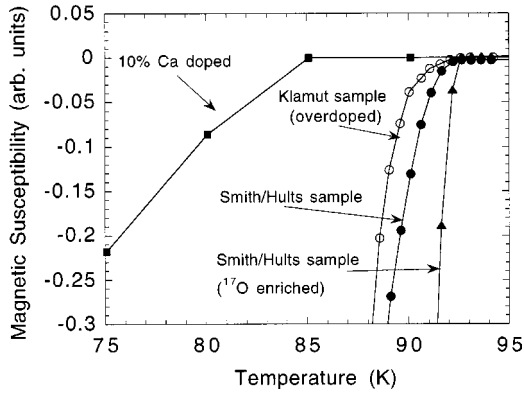


FIG. 1. Zero-field-cooled magnetic susceptibility vs temperature, as measured by dc SQUID magnetometer, for the four samples used here. Susceptibility is normalized to  $-1$  at low temperature. For sample A (Smith/Hults,  $^{17}\text{O}$  enriched) we extract transition temperature  $T_c=93$  K. For sample B (Smith/Hults) we find  $T_c=92.5$  K. Sample C (Klamut/Dabrowski) is intentionally overdoped using the procedure described in the text. We find  $T_c=91.5$  K. Sample D (Baumgartner/Lemberger, 10% Ca doped) is heavily overdoped with 10% Ca substituted for Y, and displays a broad transition at  $T_c=85$  K.

sample used in Refs. 5 and 6. We refer to this sample as ‘‘sample B (Smith/Hults).’’

Sample C was prepared by Klamut/Dabrowski (Northern Illinois University) in a manner to achieve higher oxygen content than that found in samples A and B. Sample C was synthesized from stoichiometric mixture of  $\text{Y}_2\text{O}_3$ ,  $\text{BaCO}_3$ , and a powder of 100% enriched  $^{65}\text{Cu}$  using a wet-chemistry method. Reagents were dissolved in nitric acid at room temperature. Ammonium hydroxide and citric acid were added to obtain complex citrate solution,  $\text{pH}\sim 5$ . Solution was dried at  $300^\circ\text{C}$  and decomposed in air at  $600^\circ\text{C}$ . Sintering was done in air at  $850^\circ\text{C}$ . Sample was pressed into pellets and fired in flowing oxygen at  $950^\circ\text{C}$  followed by a fast cooling to room temperature. High-pressure oxygen annealing was done in pure oxygen at 240 atm and  $250^\circ\text{C}$  for 5 days. The wet-chemistry method leads to a dense sample with homogeneous mixing of metal ions. Sample C showed a clean x-ray-diffraction pattern with sharp peaks corresponding to an orthorhombic structure. We refer to this sample as ‘‘sample C (Klamut/Dabrowski).’’

Sample D was prepared by Baumgartner/Lemberger (Ohio State University) following procedures developed by Tallon *et al.*,<sup>12</sup> and has composition  $\text{Y}_{0.9}\text{Ca}_{0.1}\text{Ba}_2\text{Cu}_3\text{O}_{7-\delta}$ , where the Ca doping is used in order to ‘‘overdope’’ the sample with extra carriers. This Ca enrichment decreases the superconducting transition temperature to  $\sim 85$  K (see below) and broadens the transition. We refer to this sample as ‘‘sample D (Baumgartner/Lemberger).’’ Measurements on sample D were reported in Ref. 13.

Figure 1 shows the zero-field-cooled magnetic susceptibility vs temperature, as measured by dc superconducting quantum interference device (SQUID) magnetometer, for each of the four samples. Even though the samples, with perhaps the exception of sample D (Baumgartner/Lemberger, 10% Ca doped), may be described as ‘‘near optimally

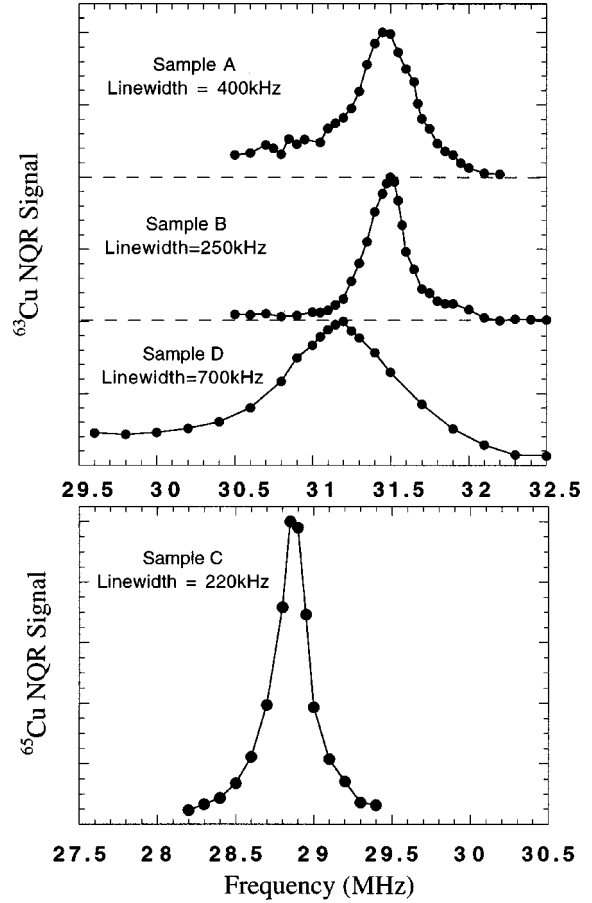


FIG. 2. Nuclear quadrupole resonance (NQR) line shapes for (top to bottom) sample A (Smith/Hults,  $^{17}\text{O}$  enriched) and sample B (Smith/Hults)-measured at 100 K, and for sample D (Baumgartner/Lemberger, 10% Ca doped) and sample C (Klamut/Dabrowski)-measured at 295 K. For the three samples at the top of the figure, the  $^{63}\text{Cu}$ NQR transition is shown. Sample C, however, is made using  $^{65}\text{Cu}$  only, and thus the  $^{65}\text{Cu}$  transition is used (the quadrupole moment of  $^{65}\text{Cu}$  is some 8% lower than that of  $^{63}\text{Cu}$ ).

doped,’’ their superconducting transitions are quite different. The widths of the transitions vary from sample to sample and the onsets of superconductivity change between being the highest ( $\sim 93$  K) for sample A (Smith/Hults,  $^{17}\text{O}$  enriched) and the lowest ( $\sim 85$  K) for sample D (Baumgartner/Lemberger, 10% Ca doped).

The differences between the physical characteristics of our samples are evidenced further in Fig. 2 in which nuclear quadrupole resonance (NQR) line shapes measured on all four samples are compared. The full width at half maximum (FWHM) of planar copper NQR line in  $\text{YBa}_2\text{Cu}_3\text{O}_{7-\delta}$ , is commonly considered to be the indicator of sample’s oxygen content and homogeneity.<sup>14</sup> Highly homogeneous samples with oxygen content close to  $\delta=0$  are expected to have relatively narrow NQR linewidth with FWHM  $\sim 250$  kHz or lower. For sample A (Smith/Hults,  $^{17}\text{O}$  enriched) the NQR linewidth is somewhat broad, FWHM  $\sim 400$  kHz, perhaps resulting from the procedure used to enrich in  $^{17}\text{O}$ . The enrichment in  $^{17}\text{O}$  has been previously shown to result in broadening of NQR lines.<sup>11</sup> The NQR linewidths of sample B (Smith/Hults) and sample C (Klamut/Dabrowski) are very

narrow, FWHM  $\sim 250$  kHz and FWHM  $\sim 220$  kHz, respectively, indicating small spreads in the distribution of electric-field gradients and high homogeneity. Sample D (Baumgartner/Lemberger, 10% Ca doped) has the broadest NQR line width, FWHM  $\sim 700$  kHz. Presumably this large linewidth results from the disorder associated with Ca doping.

### III. EXPERIMENTAL METHODS

The NMR measurements of  ${}^{63}(T_1T)^{-1}$  reported here were performed using the inversion recovery method applied to satellite transitions of  ${}^{63}\text{Cu}$  or  ${}^{65}\text{Cu}$ , with the applied field parallel to the  $c$  axis of the aligned powder samples. This method of measurement on the satellite transition, described in Ref. 3, is crucial to precision measurement. Here we present an additional demonstration of the reliability of that technique. Additionally we describe the precision methods of temperature monitoring and control that were used.

The importance of the satellite  $T_1$  measurement technique (to be defined below) is that it enables a ‘‘pure’’  $T_1$  measurement on a single isotope of Cu, a single transition of the spin- $\frac{3}{2}$  nucleus, a specific Cu site within the unit cell (i.e., plane Cu and not chain Cu), and with a unique orientation of the magnetic field with respect to the crystallographic axes. If the NMR signal monitored were not pure as defined above, the  $T_1$  measurement would not be reliable, and indeed one might expect that the results inferred would have spurious field dependence.

Fortunately the NMR parameters that determine the plane and chain  ${}^{63}\text{Cu}$  and  ${}^{65}\text{Cu}$  line shapes are well known.<sup>15</sup> At the applied magnetic field of 8.8 T one expects for a fully *unaligned* sample to find NMR signal intensity throughout the full frequency range from 69.1 to 136.6 MHz. Perfectly aligned samples with an 8.8-T field applied along the  $c$  axis yield a finite set of sharp peaks within that range. Ideally, the intensity in a given peak would be pure. Inevitably, however, alignment is not perfect, and so ‘‘aligned’’ samples yield sharp peaks, but with background intensity associated with misaligned crystallites. For a field of 8.8 T, however, the frequency of 136.6 MHz is the highest at which NMR intensity can be found. Moreover, intensity at that frequency can result only from the  ${}^{65}\text{Cu}$  ( $\frac{3}{2}, \frac{1}{2}$ ) satellite, with the field parallel to the crystallite  $c$  axis. Any misalignment can only result in a lowered frequency. Thus the signal at 136.6 MHz is pure and arises solely from planar  ${}^{65}\text{Cu}$  in crystallites that have  $c$ -axis orientations parallel to the applied field. For fields other than 8.8 T, fully analogous pure signals can be found, and in each case we have chosen the appropriate frequency for measurement. For example, for the field 14.7 T we chose the low-frequency  ${}^{63}\text{Cu}$  at 137.6 MHz, which is the *lowest* possible Cu NMR signal frequency that can occur for  $\text{YBa}_2\text{Cu}_3\text{O}_7$ .

Figure 3 displays the measured  ${}^{65}\text{Cu}$  satellite ( $\frac{3}{2}, \frac{1}{2}$ ) transition of sample B (Smith/Hults) at 8.8 T and near 136.6 MHz. Also shown are the results of measurements of  ${}^{63}(T_1)^{-1}$  at frequencies 136.55, 136.45, and 136.35 MHz, which sample both the center and the periphery of the line shape. If a background problem were present, one would

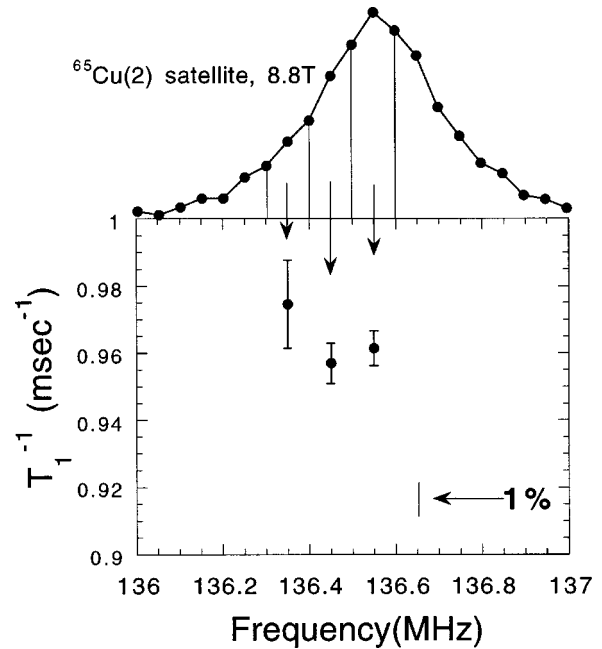


FIG. 3.  $T_1$  as measured at several frequencies within the high frequency  ${}^{65}\text{Cu}(\frac{3}{2}, \frac{1}{2})$  satellite of sample B. The applied field is 8.8 T. At this field finite signal intensity can be found in the full range from 69.1 to  $\sim 136.6$  MHz. However, intensity appearing near 136.6 MHz arises solely at the from planar  ${}^{65}\text{Cu}$  in crystallites that have  $c$  axis orientations parallel to the applied field. The measured  $T_1$  is shown to be uniform within  $\sim 1\%$  for all frequencies near 136.6 MHz. Measurement at this high-frequency satellite contrasts with measurement on the central transition, where signal intensity may arise from more than one crystallographic location and/or crystallite orientation.

expect that the measured  $T_1$  might depend strongly on the location within the line shape, since the background would be expected to be more important at the periphery of the line shape. That is not the case here. Figure 3 demonstrates that the measured  ${}^{63}(T_1)^{-1}$  is frequency independent within experimental precision of  $\sim 1\%$ . This, along with evidence discussed in Ref. 3, demonstrates that the satellite measurement method outlined here is both necessary and sufficient for reliable  $T_1$  measurements.  $T_1$  measurements were performed using the inversion recovery sequence. Figure 4 shows typical  ${}^{65}\text{Cu}$  recovery curves obtained using the high-frequency  ${}^{65}\text{Cu}$  ( $\frac{3}{2}, \frac{1}{2}$ ) satellite of sample C (Klamut/Dabrowski) at 8.8 T, for a temperature above (94.5 K) and below (69.8 K)  $T_c$ . Along with the experimental data is shown the expected functional form for the recovery  $[M(t) - M_o(t)] \propto [0.1e^{-t/T_1} + 0.5e^{-3t/T_1} + 0.4e^{-6t/T_1}]$ , using best fit  $T_1$ 's for the respective temperatures.

A second experimental concern for precise  $T_1$  measurement is temperature monitoring and control. The sample probe is inserted into an Oxford CF1200 He gas-flow cryostat, which itself is inserted in the room-temperature bore of the 8.8 T superconducting magnet. The CF1200 monitors and controls temperature in the cryostat. We found it necessary though to monitor the sample temperature separately using a Cernox X0 8403 thermometer mounted inside the probe at a distance of  $\sim 1$  cm from the sample. Temperature

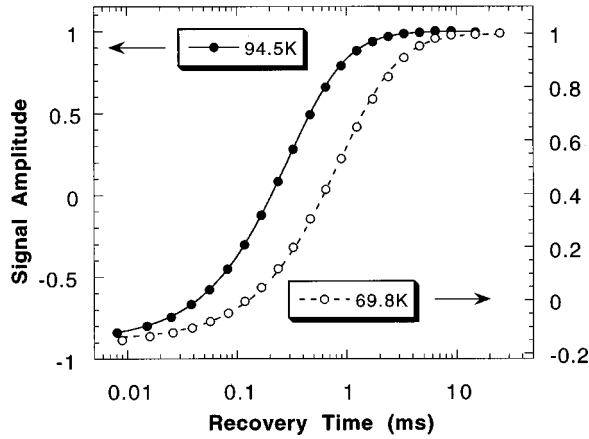


FIG. 4. Typical  $^{65}\text{Cu}$  spin lattice relaxation data obtained using the high-frequency  $^{65}\text{Cu}(\frac{3}{2}, \frac{1}{2})$  satellite of sample C (Klamut/Dabrowski) at 8.8 T. Data were obtained using the inversion recovery sequence. Closed circles represent recovery data obtained at 94.5 K (normal state) and the opened circles represent data obtained at 69.8 K (superconducting state). The experimental results were fit to the corresponding functional form:  $[M(t) - M_o(t)] \propto [0.1e^{-t/T_1} + 0.5e^{-3t/T_1} + 0.4e^{-6t/T_1}]$ , yielding  $^{65}(T_1)^{-1} = 0.821 17 \pm 0.002 274 3$  at 94.5 K and  $^{65}(T_1)^{-1} = 0.278 12 \pm 0.003 493 9$  at 69.8 K. The fits are given by the solid and the dashed line for 94.5 and 69.8 K, respectively. The superconducting state measurement displays a more incomplete inversion, presumably because supercurrents are effective in partially screening the applied rf inversion pulse.

vs time for the sample was monitored throughout the measurements of  $T_1$  reported here. Figure 4 shows temperature vs time during a typical  $T_1$  measurement. At the beginning of the NMR pulse sequence, the temperature rises by  $\sim 0.25$  K as a result of the rf heating from the NMR pulses. About 120 min after the start of the pulse sequence the temperature reaches a steady state, and only at that time do we begin acquiring data for the  $T_1$  measurement. As seen in Fig. 5, the temperature holds steady within 0.02 K during the  $T_1$  measurement. When the NMR pulse sequence ceases the measured temperature returns to its previous value.

#### IV. RESULTS AND CONCLUSIONS

The results of the  $^{63}(T_1 T)^{-1}$  measurements for all four samples are shown in Fig. 6, with the following symbol scheme: all of the gray-shaded symbols are from sample A (Smith/Hults,  $^{17}\text{O}$  enriched), black symbols are from sample B (Smith/Hults), and open symbols are sample C (Klamut/Dabrowski). Finally, the inset is sample D (Baumgartner/Lemberger, 10% Ca doped). The applied fields for each measurement are indicated by the *type* of symbol (as opposed to its shade), with the following scheme: squares denote 0 T, diamonds 4 T, circles 8.8 T, and triangles 14.8 T. Only normal-state data are shown in the figure, where “normal state” is defined by the condition that  $T > T_c(B)$  for the applied field used, and with  $dB_{c2}/dT = -1.9\text{T/K}$ .<sup>16</sup>

The clear outcome of Fig. 6 is that the normal state  $^{63}(T_1 T)^{-1}$  is found to be field independent with precision of  $\sim 1\%$  over the full range from 0 to 14.8 T for all samples. To

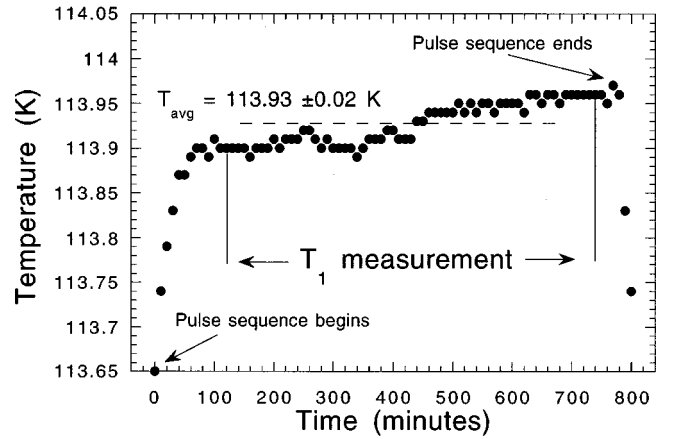


FIG. 5. Temperature vs time acquired during a typical measurement of  $T_1$ . The temperature is measured using a Cernox X0 8403 thermometer mounted inside the probe at a distance of  $\sim 1$  cm from the sample. At the beginning of the NMR pulse sequence, the temperature rises by  $\sim 0.25$  K as a result of the rf heating from the NMR pulses. About 120 min after the start of the pulse sequence the temperature reaches a steady state, and we began acquiring data for the  $T_1$  measurement. The temperature holds steady within 0.02 K during the  $T_1$  measurement.

illustrate this we plot in Fig. 7  $^{63}(T_1 T)^{-1}$  for each of the samples vs magnetic field, all for a fixed temperature of 95 K. (In cases where there was no measurement at exactly 95 K we have linearly interpolated between the data points of Fig. 6 that are closest to 95 K.) 95 K is, of course, slightly

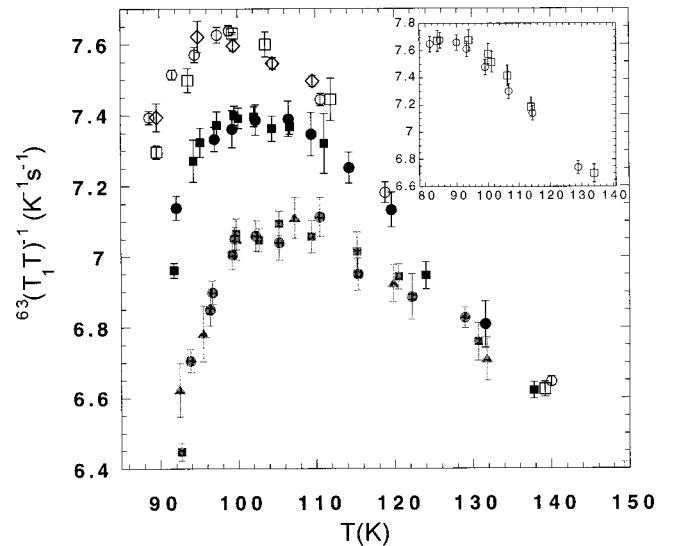


FIG. 6. Measured  $^{63}(T_1 T)^{-1}$  vs  $T$  for several samples at the following applied fields: 0 T (squares), 4 T (diamonds), 8.8 T (circles), and 14.8 T (triangles). Gray points are from sample A (Smith/Hults,  $^{17}\text{O}$  enriched). Black points are from sample B (Smith/Hults). Open points are sample C (Klamut/Dabrowski). Inset is sample D (Baumgartner/Lemberger, 10% Ca doped). Only normal state data are shown in the figure, where “normal state” is defined by the condition that  $T > T_c(B)$  for the applied field used.  $^{63}(T_1 T)^{-1}$  is found to be field independent with precision of  $\sim 1\%$  over the full range from 0 to 14.8 T. Below  $T_c(B)$ , however, the data “fan out,” as expected, and as shown in Fig. 8.

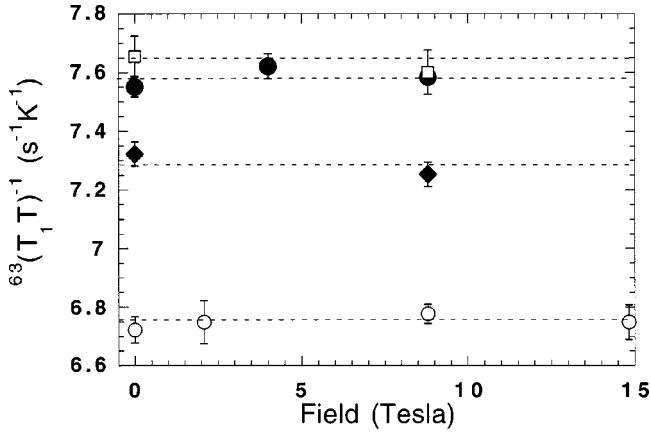


FIG. 7.  ${}^{63}(T_1T)^{-1}$  vs applied field  $B$ , at temperature 95 K. Open circles: sample A (Smith/Hults,  ${}^{17}\text{O}$  enriched). Closed diamonds: sample B (Smith/Hults). Closed circles: sample C (Klamut/Dabrowski). Open squares: sample D (Baumgartner/Lemberger 10% Ca doped). For each sample  ${}^{63}(T_1T)^{-1}$  is shown to be independent of field within experimental error as shown.

above  $T_c$ . We select that temperature, first because it is the temperature range at which the “spin gap” effects (discussed below) are most pronounced, and second because it is also the temperature at which Mitrovic *et al.*<sup>4</sup> report the strongest field dependence. Below  $T_c(B)$  the data to begin to exhibit field dependence and  ${}^{63}(T_1T)^{-1}$  increases with  $B$ , as shown in Fig. 8 for two of our samples.

From Figs. 6 and 7 we see that for *all* samples reported here the quantity  ${}^{63}(T_1T)^{-1}$  is field independent. We stress that these samples, despite having  $T_c$ 's above 90 K (except for sample D), appear from Figs. 1 and 2 to be quite different

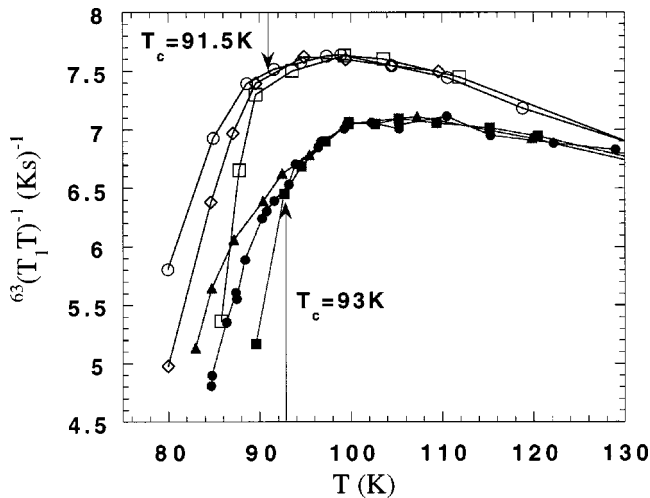


FIG. 8.  ${}^{63}\text{Cu}{}^{63}(T_1T)^{-1}$  vs temperature for several magnetic fields and for two samples. All open symbols are for sample C (Klamut/Dabrowski). All filled symbols are for sample A (Smith/Hults  ${}^{17}\text{O}$  enriched). Squares indicate zero magnetic field; diamonds indicate 4 T; circles 8.8 T, and triangles 14.8 T. Also indicated by arrows on the plot are the zero-field transition temperatures for each sample. While there is no field dependence above  $T_c(B=0)$ , a clear field dependence does develop, as expected, for temperatures below  $T_c(B=0)$ .

in their detailed doping level and/or degree of disorder. Both samples C (Klamut/Dabrowski) and D (Baumgartner/Lemberger) are prepared to be “overdoped,” sample C through high-pressure oxygen anneal and D through Ca substitution. Furthermore the temperature dependences (as opposed to field dependences) of  ${}^{63}(T_1T)^{-1}$  are quite different for the four samples. All samples except D display the beginnings of a sharp downturn in  ${}^{63}(T_1T)^{-1}$  with decreasing temperature, for temperatures well above  $T_c$ . That downturn is what is termed the spin gap effect. However, the overdoped samples C and D display a much less prominent downturn. Mitrovic *et al.* previously<sup>9</sup> suggested that the sharp downturn observed in our sample A and reported in Ref. 3 indicated that our sample was underdoped. They suggested at the time that the field dependence that they had observed might only appear in “high-quality optimally doped materials.” [Again, though, they now report<sup>10</sup> that the apparent field dependence of  ${}^{63}(T_1T)^{-1}$ , which they inferred indirectly from their  ${}^{17}\text{O}$   $T_2$  measurements, does not occur in their own direct measurements of  ${}^{63}(T_1T)^{-1}$ .] Figures 6 and 7 show very clearly that although the details of the sample affect the temperature dependence of  ${}^{63}(T_1T)^{-1}$ , they do not change the finding of field independence. Our data is remarkably consistent with the recent field-dependence measurements of Zheng *et al.*<sup>17</sup> in the underdoped material,  $\text{YBa}_2\text{Cu}_4\text{O}_8$ , where these authors also found  ${}^{63}(T_1T)^{-1}$  to be field independent in the normal state and enhanced with field in the superconducting state. [These authors have more recently<sup>18</sup> measured  ${}^{63}(T_1T)^{-1}$  in  $\text{TlSr}_2\text{CaCu}_2\text{O}_{6.8}$  and found field dependence below and up to a few degrees above their measured  $T_c(H)$ .]

In conclusion, the final clear result of magnetic field independence of  ${}^{63}(T_1T)^{-1}$  is identical to that of Ref. 3. Regarding the issue of the field dependence or independence of the spin gap effect, we have little to add to the theoretical discussion provided in that reference. Even to this date, it yet appears that there are no quantitative calculations of spin gap field dependence. Our result does, however, impact on the theoretical discussion of Mitrovic *et al.*<sup>4</sup> in which they evoked a model of *d*-wave superconducting fluctuations that accurately reproduced their data. Surely superconducting fluctuations exist, and so we presume that the model is applicable. We speculate that the model must allow a range of adjustable parameters that could encompass either their findings of strong field dependence or the current consensus finding of field independence.

#### ACKNOWLEDGMENTS

This work was supported by the National Science Foundation Division of Materials Research Contract No. NSF/DMR-9972200 (Pennington group), by DARPA/ONR and State of Illinois under HECA (Dabrowski group), and by DOE Grant No. DEFG02-90ER45427 through the Midwest Superconductivity Consortium (Lemberger group). Work at Los Alamos was performed under the auspices of the U.S. Department of Energy.

- <sup>1</sup>F. Borsa, A. Rigamonti, M. Corti, J. Ziolo, O.-B. Hyun, and D. R. Torgeson, *Phys. Rev. Lett.* **68**, 698 (1992).
- <sup>2</sup>P. Carretta, D. V. Livanov, A. Rigamonti, and A. A. Varlamov, *Phys. Rev. B* **54**, 9682 (1996).
- <sup>3</sup>K. R. Gorny, O. M. Vyaselev, J. A. Martindale, V. A. Nandor, C. H. Pennington, P. C. Hammel, W. L. Hults, J. L. Smith, P. L. Kuhns, A. P. Reyes, and W. G. Moulton, *Phys. Rev. Lett.* **82**, 177 (1999).
- <sup>4</sup>V. F. Mitrovic, H. N. Bachmann, W. P. Halperin, M. Eschrig, J. A. Sauls, A. P. Reyes, P. Kuhns, and W. G. Moulton, *Phys. Rev. Lett.* **82**, 2784 (1999).
- <sup>5</sup>C. H. Recchia, K. R. Gorny, and C. H. Pennington, *Phys. Rev. B* **54**, 4207 (1996).
- <sup>6</sup>C. H. Recchia, J. A. Martindale, C. H. Pennington, W. L. Hults, and J. L. Smith, *Phys. Rev. Lett.* **78**, 3543 (1997).
- <sup>7</sup>R. E. Walstedt and S.-W. Cheong, *Phys. Rev. B* **51**, 3163 (1995).
- <sup>8</sup>R. E. Walstedt and S.-W. Cheong, *Phys. Rev. B* **53**, R6030 (1996).
- <sup>9</sup>V. F. Mitrovic, H. N. Bachmann, W. P. Halperin, M. Eschrig, and J. A. Sauls, cond-mat/9901232 (unpublished).
- <sup>10</sup>W. P. Halperin, *Bull. Am. Phys. Soc.* **45**, 400 (2000).
- <sup>11</sup>J. A. Martindale, Ph.D. thesis, University of Illinois, Urbana, Illinois, 1993.
- <sup>12</sup>J. L. Tallon, C. Bernhard, H. Shaked, R. L. Hitterman, and J. D. Jorgensen, *Phys. Rev. B* **51**, 12 911 (1995).
- <sup>13</sup>K. R. Gorny, O. M. Vyaselev, J. A. Martindale, J. A. Skinta, C. H. Pennington, J. E. Baumgartner, and T. R. Lemberger, *Bull. Am. Phys. Soc.* **43**, 966 (1998).
- <sup>14</sup>A. J. Vega, W. E. Farneth, E. M. McCarron, and R. K. Bordia, *Phys. Rev. B* **39**, 2322 (1989).
- <sup>15</sup>C. H. Pennington, D. J. Durand, C. P. Slichter, J. P. Rice, E. D. Bukowski, and D. M. Ginsberg, *Phys. Rev. B* **39**, 2902 (1989).
- <sup>16</sup>U. Welp, W. K. Kwok, G. W. Crabtree, K. G. Vandervoort, and J. Z. Liu, *Phys. Rev. Lett.* **62**, 1908 (1989).
- <sup>17</sup>G. Zheng, W. G. Clark, Y. Kitaoka, K. Asayama, Y. Kodama, P. Kuhns, and W. G. Moulton, *Phys. Rev. B* **60**, 9947 (1999).
- <sup>18</sup>G. Zheng, H. Ozaki, W. G. Clark, Y. Kitaoka, P. Kuhns, A. P. Reyes, W. G. Moulton, T. Kondo, Y. Shimakawa, and Y. Kubo, *Phys. Rev. Lett.* **85**, 405 (2000).